Inorganic Chemistry

pubs.acs.org/IC
Article

Synthesis of the Bulky Phosphanide $[P(Si^iPr_3)_2]^-$ and Its Stabilization of Low-Coordinate Group 12 Complexes

Olivia P. Churchill,[‖] Antonia Dase,[‖] Laurence J. Taylor, Stephen P. Argent, Nathan T. Coles, Gavin S. Walker, and Deborah L. Kays*

Cite This: *Inorg. Chem.* 2024, 63, 20286−20294

ABSTRACT: Here, we report an improved synthesis of the bulky phosphanide anion $[P(Si^iPr_3)_2]^-$ in synthetically useful yields and its complexation to group 12 metals. The ligand is obtained as the sodium salt $NaP(Si^iPr_3)_2$ **1** in a 42% isolated yield and a single step from red phosphorus and sodium. This is a significantly higher-yielding and safer preparation compared to the previously reported synthesis of this ligand, and we have thus applied **1** to the synthesis of the two-coordinate complexes $M[P(Si^iPr_3)_2]_2$ (M = Zn, Cd, Hg). These group 12 complexes are all monomeric and with nonlinear P−M−P angles in the solid state, with DFT calculations suggesting that this bending is due to the steric demands of the ligand. Multinuclear NMR spectroscopy revealed complex second-order splitting patterns due to strong PP' coupling. This work demonstrates that the synthesis of **1** is viable and provides a springboard for the synthesis of low-coordinate complexes featuring this unusual bulky ligand.

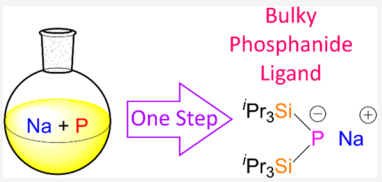

INTRODUCTION

The use of sterically demanding ligands to enforce low-coordination geometries upon d- and f-block metal centers remains an area of interest for inorganic chemists.[1−7] Such complexes are typically highly reactive and thus capable of acting as a catalyst or a reagent for small molecule reactivity and activation.[3,8−17] These complexes can also display single molecule magnet (SMM) behavior.[18−27] The use of amides as versatile, sterically demanding ligands dates to the 1960s, with the use of the $[N(SiMe_3)_2]^-$ ligand to isolate first the alkali metal silylamides, then the homoleptic $Al[N(SiMe_3)_2]_3$ and $Sn[N(SiMe_3)_2]_2$ complexes, as well as several two-coordinate d-block complexes.[28−34] Since then, a wide array of bulky silylamide ligands such as $[N(Dipp)(SiMe_3)]^-$, $[N(SiHMe_2)_2]^-$, and $[N(SiPh_2Me)_2]^-$ have been developed and utilized in complexation reactions with metals across the periodic table.[4,16,35−44] More recently, the exceedingly bulky $KN(Si^iPr_3)_2$ has been applied to the synthesis of linear f-block species, which display large magnetic anisotropy and have the potential for extremely high U_{eff} values (U_{eff} = barrier to magnetization),[45−47] as well as group 2 Lewis acidic cations.[48] Most recently, investigations of $(^tBu_3Si)_2NH$ showed the amine to be resistant to deprotonation even by ^{n}BuLi/KO^{t}Bu superbase mixtures. However, the coordination of $[N(Si^tBu_3)_2]^-$ to Cs was achieved through the reaction of $(^tBu_3Si)_2NH$ with Cs^0/THP electride solution (THP = tetrahydropyran). The resulting $Cs(NSi^tBu_3)_2$ complex was shown to undergo a metathesis reaction when reacted with LiI.[49]

While bulky silylamides are relatively well established, the corresponding phosphorus analogues have received considerably less attention. Previous studies of the $[P(SiMe_3)_2]^-$ ligands have afforded dimeric or polymeric structures. The substitution reactions between $M[N(SiMe_3)_2]_2$ (M = Zn, Cd, Hg, Sn, Pb, and Mn) with two equivalents of $(Me_3Si)_2PH$ lead to the formation of the dimeric $[M(P(SiMe_3)_2\{\mu_2\text{-}P(SiMe_3)_2\}]_2$ complexes. In the case of the reaction with manganese, $(THF)Mn[N(SiMe_3)_2]$ was used and the resulting phosphanide complex contained a three-coordinate and a four-coordinate manganese center bearing one THF ligand.[50] Dimeric $Li(THF)_2P(SiMe_3)_2$, tetrameric $Li(THF)_{0.5}P(SiMe_3)_2$, and hexameric $LiP(SiMe_3)_2$ complexes were prepared from the reaction of $P(SiMe_3)_3$ with ^{n}BuLi in THF or cyclopentane,[51,52] while polymeric, ladder-type structures of the heavier alkali metals with the general formula $[(THF)AP(SiMe_3)_2]_\infty$ (A = K, Rb, Cs) were prepared from the reaction of $P(SiMe_3)_3$ with the corresponding alkali metal *tert*-butoxide (AO^tBu).[53] To the best of our knowledge, the only two-coordinate metal bis(silylphosphanido) complexes to date are $M[P(SiPh_3)_2]_2$ (M = Zn, Cd, Hg), prepared by Matchett et al.[54] Here, the higher steric demands of the $-SiPh_3$ group offset the larger P atom, allowing for the isolation of monomeric species. Thus, we propose that the phosphorus analogue of the aforementioned $[N(Si^iPr_3)_2]^-$ ligand is of considerable interest due to its steric bulk, which should allow the isolation of monomeric complexes. While the $[P(Si^iPr_3)_2]^-$ ligand is known, it has scarcely been studied due to difficulties

Received: July 24, 2024
Revised: September 13, 2024
Accepted: October 1, 2024
Published: October 10, 2024

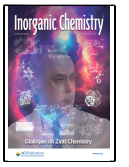

https://doi.org/10.1021/acs.inorgchem.4c03134
Inorg. Chem. 2024, 63, 20286−20294

in its preparation. Westerhausen et al. prepared the Li salt $[(THF)LiP(Si^iPr_3)_2]_2$ by first reacting ^{n}BuLi with PH_3 in the presence of DME (DME = 1,2-dimethoxyethane) to obtain $(DME)LiPH_2$ in an 82−91% yield.[55,56] This was then reacted with ^{i}Pr$_3$SiCl to afford ^{i}Pr$_3$SiPH$_2$ (64%), with $(^i$Pr$_3$Si$)_2$PH obtained as a minor byproduct (13%).[57] Further reaction of the minor product $(^i$Pr$_3$Si$)_2$PH with ^{n}BuLi in THF afforded $[(THF)LiP(Si^iPr_3)_2]_2$ in an 83% yield,[58] giving an overall yield from PH_3 of at most 9.8%. Given the difficult and low-yielding synthesis, $[(THF)LiP(Si^iPr_3)_2]_2$ was used to prepare only one complex, $[(THF)_4Li][(^iPr_3Si)_2PW(CO)_5]$. As such, the potential of this ligand is largely unexplored.

Herein, we present a much-improved synthesis of an alkali metal complex of this ligand, the Na^+ salt $NaP(Si^iPr_3)_2$ (**1**), which was obtained in a 42% isolated yield and in a single step. This has allowed us to prepare the family of group 12 complexes $M[P(Si^iPr_3)_2]_2$ (M = Zn (**2**), Cd (**3**), Hg (**4**)), by salt metathesis reactions, demonstrating the synthetic utility of this ligand precursor.

RESULTS AND DISCUSSION

Synthesis of NaP(Si^{i}Pr$_3$)$_2$ 1. To obtain a more direct route to the $[P(Si^iPr_3)_2]^-$ anion than previously reported,[58] we looked to the synthesis of $P(Si^iPr_3)_3$ published by von Hänisch. Here, red phosphorus was reacted with NaK in refluxing DME to generate $(Na/K)_3P$, which was subsequently reacted with ^{i}Pr$_3$SiCl.[59] Since $P(SiMe_3)_3$ can be converted to $(Me_3Si)_2PH$ by hydrolysis or methanolysis,[60,61] we postulated that it could be possible to obtain $(^i$Pr$_3$Si$)_2$PH in a similar manner. However, the use of a highly pyrophoric NaK alloy was a safety concern. To mitigate this, we instead used Na with 10 mol % naphthalene as an electron-transfer agent.[62] This method has been used previously to generate Na_3P *in situ*[63,64] for the preparation of tris(trimethylsilyl)phosphine, $P(SiMe_3)_3$.[65]

In our initial testing, we found that it was necessary to reflux the Na/naphthalene and red phosphorus for 24 h in DME; otherwise, the resulting product contained significant amounts of unreacted ^{i}Pr$_3$SiCl and $(^i$Pr$_3$Si$)_2$. This is believed to occur due to the incomplete formation of Na_3P and the presence of unreacted Na. When monitoring the reaction by ^{31}P NMR spectroscopy, we found that a mixture of P-containing species was formed, including $P(Si^iPr_3)_3$ and $(^i$Pr$_3$Si$)_2$PH, which were identified by comparison with the literature.[58] Another significant ^{31}P NMR signal was observed at −378 ppm (compound **1**). By removing the DME *in vacuo*, then extracting the resulting residue in hexane or toluene, it was possible to precipitate **1** from the reaction mixture as a white pyrophoric solid, while $P(Si^iPr_3)_3$, $(^i$Pr$_3$Si$)_2$PH, and other P-containing byproducts remained in solution. ^{1}H, ^{13}C{^{1}H}, ^{31}P, and ^{31}P{^{1}H} NMR spectroscopy of **1** suggested that the complex contained a $-P(Si^iPr_3)_2$ moiety with minor residual solvent peaks (see Supporting Information Figures S2 and S3). While it was not possible to obtain crystals of **1** suitable for single-crystal X-ray diffraction studies, crystals of $[(THF)NaP(Si^iPr_3)_2]_2$ (**1a**) were obtained when a reaction mixture containing **1** was dissolved in C_6D_6 and THF (Figure 1) and left at room temperature for 4 weeks. Based on this structure and the NMR spectroscopic data, we propose that **1** corresponds to $NaP(Si^iPr_3)_2$. Due to the very high sensitivity of **1**, it was not possible to obtain high-resolution mass spectrometric data on this compound.

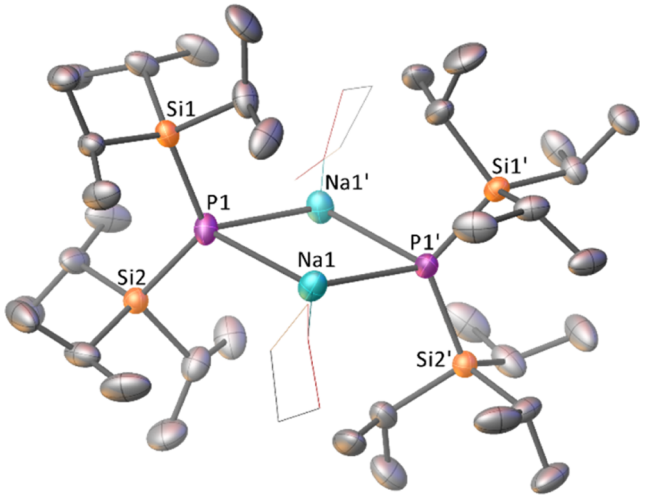

Figure 1. Single-crystal X-ray diffraction structure of $[(THF)NaP(Si^iPr_3)_2]_2$ **1a**. Coordinated THF represented as a wireframe, minor disorder components, and hydrogen atoms omitted for clarity. Thermal ellipsoids are set to the 50% probability. Atoms marked with ' are obtained using the following symmetry operation: $1-x, +y, \frac{1}{2}-z$. Selected bond lengths (Å) and angles (deg): Na1−P1 2.8039(11), Na1−P1' 2.806(1), Na−O1A 2.200(6), Na−O1B 2.203(6), Na−O1C 2.309(3), Na1●●●Na1' 3.4586(18), P1−Si1 2.2207(8), P1−Si2 2.2163(7), P1−Na1−P1' 103.84(3), Na1−P1−Na1' 76.15(3), and Si1−P1−Si2 120.56(3).

Given that our aim had been to convert $P(Si^iPr_3)_3$ to the $[P(Si^iPr_3)_2]^-$ anion via a multistep process, the observation of **1** was quite exciting. Here, we directly formed a phosphanide anion in a single step and purified it by precipitation and filtration. Thus, we focused on optimizing the synthesis to maximize the yield of **1**, rather than $P(Si^iPr_3)_3$. This led to the development of the methodology shown in Scheme 1. Note that attempts with a 2:1 stoichiometry of ^{i}Pr$_3$SiCl:Na_3P resulted in an increase in the quantity of $(^i$Pr$_3$Si$)_2$PH produced relative to the desired $NaP(Si^iPr_3)_2$ (only 13% $NaP(Si^iPr_3)_2$ observed by ^{31}P NMR of the crude reaction mixture); thus, a 3:1 reaction stoichiometry was found to perform best. Na and 10 mol % naphthalene were refluxed in DME for 24 h, after which ^{i}Pr$_3$SiCl was added and the reaction was heated for a further 24 h. After filtration to remove insoluble impurities, the DME was removed *in vacuo*, and the resulting oil was extracted into toluene. This precipitated **1**, which was isolated by filtration in a 42% yield with sufficient purity for further synthesis. The crude reaction mixture showed the formation of **1**, $(^i$Pr$_3$Si$)_2$PH, and $P(Si^iPr_3)_3$ in an approximate 1:0.28:0.08 ratio (see Supporting Information Figure S6). As $(^i$Pr$_3$Si$)_2$PH has been previously shown to be readily converted to $[(THF)LiP(Si^iPr_3)_2]_2$,[58] which can also be used in transmetalation reactions, it is suggested that isolation of this byproduct would further increase the yield of usable phosphanide precursors from this reaction. Note that, concurrent with our reported work, the Mills group has developed a similar (albeit lower-yielding) synthesis of **1**.[66]

Synthesis of Group 12 Complexes 2−4. The two-coordinate group 12 complexes **2**−**4** were prepared by the metathesis reaction of **1** with the appropriate metal halide ($ZnCl_2$, CdI_2, and $HgBr_2$) in diethyl ether (Scheme 2). The resulting complexes were isolated as white crystalline solids in moderate to good yields (40−57%) after extraction and recrystallization from *n*-hexane. For the formation of **3**, it was

https://doi.org/10.1021/acs.inorgchem.4c03134
Inorg. Chem. 2024, 63, 20286−20294

Scheme 1. Optimized Synthesis of $NaP(Si^iPr_3)_2$ (1)

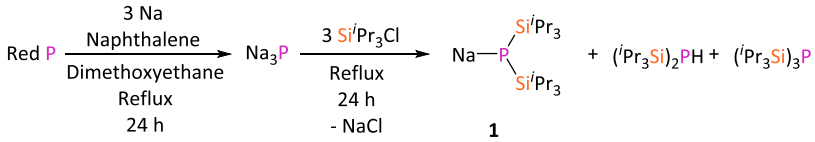

Scheme 2. Synthesis of Group 12 Bis(silylphosphanido) Complexes 2−4. MX_2 = $ZnCl_2$, CdI_2, $HgBr_2$

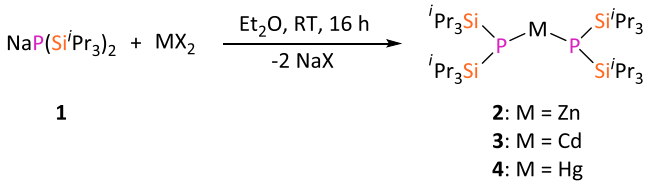

necessary to use CdI_2, as reactions between **1** and $CdCl_2$ in diethyl ether led to precipitation of Cd(0). Complexes **2**−**4** are air- and moisture-sensitive and were characterized by single-crystal X-ray diffraction and multinuclear NMR spectroscopy. Complex **2** was also characterized by HRMS and CHN microanalysis; the high toxicity of complexes **3** and **4** precluded their analysis by these methods.

Crystals of **2**−**4** suitable for single-crystal X-ray diffraction were obtained from the storage of saturated *n*-hexane solutions at −30 °C (Figure 2). A polymorph structure of **2** (**2a**) was also obtained by slow evaporation from diethyl ether (Figure S1). **2** and **2a** crystallize in the same space group ($P\bar{1}$) but with a different unit cell (Table S1) and with significantly different P1−Zn1−P2 angles [168.747(12)° vs 163.593(18)°]. All structures show **2**−**4** to be monomeric and two-coordinate in the solid state. The M1−P1 and M1−P2 bond lengths (Table 1) are similar to those seen in the terminal silylphosphanido groups in $[M(P(SiMe_3)_2\{\mu_2\text{-}P(SiMe_3)_2\})]_2$ (Zn−P_t 2.295(1) Å, Cd−P_t 2.459(1) Å, and Hg−P_t 2.402(1) Å).[50] The P−Si bond lengths differ slightly between complexes [2.2479(4)−2.2657(8) Å; Table 1] but are consistent with P−Si single bonds, with little evidence of the P−Si double bond character [typical P=Si distances 2.062(1)−2.158(2) Å].[67] The sum of the angles around each phosphorus center ($\sum°$; Table 1) is also consistent with an sp^3-hybridized P atom (*i.e.* no P=Si bond character). It has been postulated that the unusually wide Si−N−Si and Si−O−Si bond angles of the bis(silyl)amides and ethers arise from negative hyperconjugation, with increasing steric bulk of the ligands leading to a further widening of these bonds.[49] In the case of bis(triisopropylsilyl)phosphanide complexes **1a**−**4**, the Si−P−Si bond angles are more acute [117.09(15)−125.903(18)°] than those observed for the bis(triisopropylsilyl)amide lanthanide complexes $Ln[N(Si^iPr_3)_2]_2$ (typical Si−P−Si bond angles 137.6−139.8° for Ln = Sm, Eu, Tm, Yb).[45,46] An increase in the Si−P−Si bond angles arises when comparing complexes **1a** and **2**−**4** with the hexameric $[LiP(SiMe_3)_2]_6$ complex [Si−P−Si 107.8(1)−108.6(1)°][52] and the terminal silylphosphanide groups of $[M(P(SiMe_3)_2\{\mu_2\text{-}P(SiMe_3)_2\})]_2$ [Si−P_t−Si 106.2(1)° (Zn); 106.6(1)° (Cd); 107.2(1)° (Hg); 100.3(4)° (Pb); 106.6(1), 105.1(1)° (Mn)].[50] $Cd[P(SiPh_3)_2]_2$ prepared by Matchett et al. also displays a small Si−P−Si bond angle [107.7(1)°] attributed to the lack of substantial steric interactions between the $SiPh_3$ substituents.[54] The limited data for bis(silyl)phosphanide complexes hinder the ability to establish a correlation between Si−P−Si bond angles and the steric demands of the ligand. All of the complexes exhibit a nonlinear P−M−P unit, with this angle increasing from Zn > Cd > Hg (Table 1).

Computational Investigations. Given that closed-shell, two-coordinate metal complexes are frequently linear,[68−76] although nonlinear species are known,[74,77−80] and that the only previous group 12 bis(silylphosphanido) complex to be structurally characterized ($Cd[P(SiPh_3)_2]_2$) was linear,[54] DFT calculations were used to probe the reasons for the deviation from linearity for **2**−**4** in the solid state. Geometry optimizations were performed on **2**−**4** (PBE0/SARC-ZORA-TZVP for Cd and Hg, PBE0/ZORA-def2-TZVP for all other atoms).[81−88] Grimme's D3 dispersion corrections were applied to all optimizations.[89,90] The optimized structures were in good agreement with those determined experimentally and in all cases reproduced the nonlinear P−M−P (M = Zn, Cd, Hg) bond angles (Table S2). Models of **2**−**4** were also optimized with a 180° P−M−P bond angle restraint, affording linear models (**2′**, **3′**, **4′**). These linear models were found to be significantly *less* thermodynamically stable than the bent structures, with linearization energies (ΔE_{lin}) of 13.3 kcal mol^{-1} for Zn, 10.7 kcal mol^{-1} for Cd, and 8.9 kcal mol^{-1} for Hg.[77] The linear structures show a significant distortion about the P atoms, with asymmetry in the M−P−Si angles (Figure S31 and Table S2). By contrast, the M−P−Si groups in the nonlinear optimized structures were more symmetric (Figure S32 and Table S2). This suggests that the bent P−M−P bond angles are a consequence of the steric demands of the $[P(Si^iPr_3)_2]^-$ ligands. To fit these ligands around the metal, it is necessary to distort at *either* the metal center *or* the P atoms, with the distortion at the metal being more favorable. The solid-state structure of $Cd[P(SiPh_3)_2]_2$ shows relatively symmetric Cd−P−Si angles (100.9(2)°, 98.2(1)°) and a linear P−Cd−P angle,[54] suggesting that a smaller ligand removes the need for distortion. Geometry optimization (without restraints) of the less sterically demanding $Cd[P(SiMe_3)_2]_2$, starting from linear and nonlinear geometries, afforded both linear (P−Cd−P = 179.9°) and near-linear (P−Cd−P = 177.5°) molecules. These two geometries showed near-identical energies (ΔG = 0.1 kcal mol^{-1}), suggesting that there is little energetic difference between these two coordination environments for the less sterically demanding $[P(SiMe_3)_2]^-$ ligand.

NMR Spectroscopic Analysis. The $^{13}C\{^1H\}$ NMR spectra of **2**−**4** (Figure 3) and the $^{29}Si\{^1H\}$ NMR spectrum of **4** (Figure 4) show evidence of second-order effects due to strong virtual coupling between the ^{31}P nuclei ($^2J_{PP'}$). Similar effects have been reported in the literature for analogous phosphorus−carbon ABX and AA'X systems.[91−93] Despite the different appearances of the $^{13}C\{^1H\}$ NMR signals, the $^2J_{CP}$ and $^3J_{CP}$ coupling constants are similar across the series [$^2J_{CP}$ = 10.7 Hz (**2**), 10.3 Hz (**3**), 10.2 Hz (**4**); $^3J_{CP}$ = 3.6 Hz (**1**) 3.7 Hz (**2**), 3.5 Hz (**4**)]. This indicates that the differences between **2** and **4** are likely caused by the changing magnitude of $^2J_{PP'}$ across the series.

https://doi.org/10.1021/acs.inorgchem.4c03134
Inorg. Chem. 2024, 63, 20286−20294

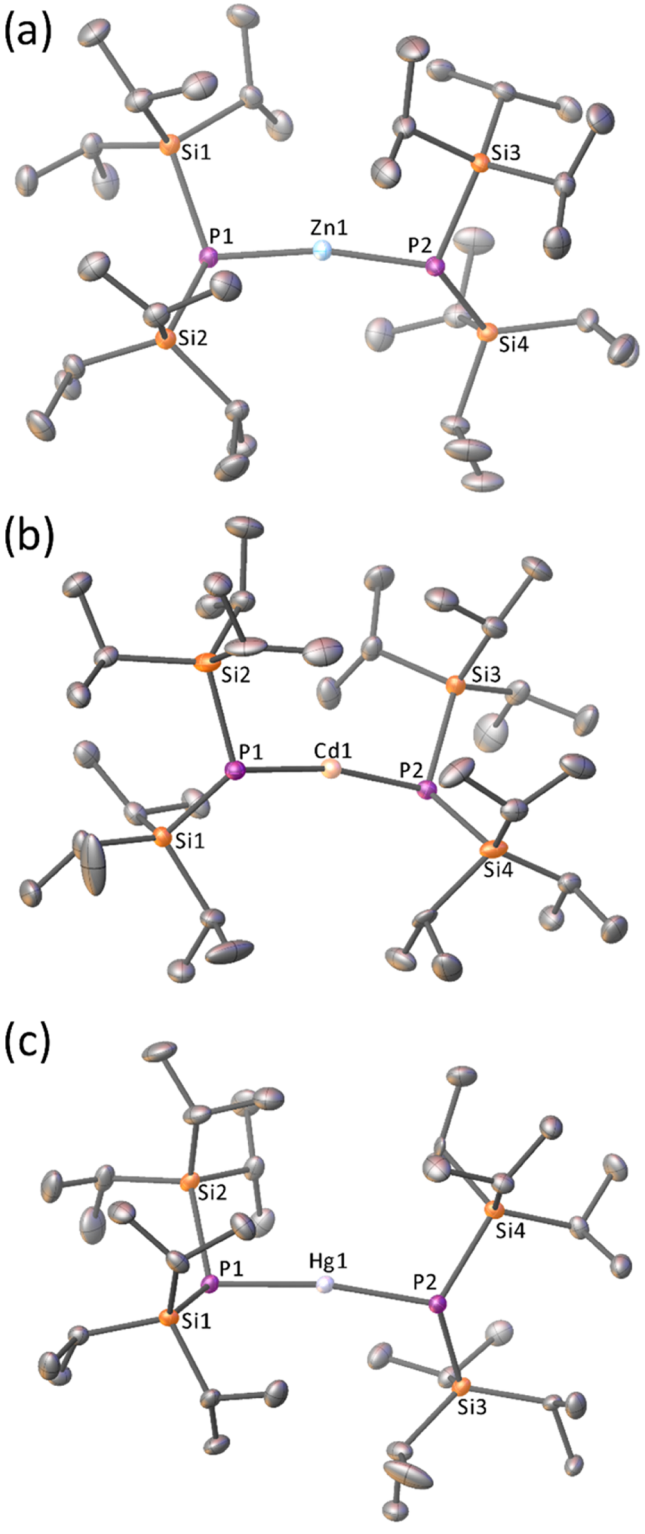

Figure 2. View of the single-crystal X-ray diffraction structures of (a) **2**, (b) **3**, and (c) **4**. Hydrogen atoms and minor disorder components of **3** and **4** have been omitted for clarity. Thermal ellipsoids are shown at a 50% probability.

While the $^{29}Si\{^{1}H\}$ NMR spectra of **2** and **3** show apparent doublets, that of **4** is more complex, consistent with an AA'X spin system with virtual coupling. This spectrum was well simulated with parameters of $^{1}J_{SiP}$ = 50.6 Hz, $^{3}J_{SiP'}$ = 0.0 Hz, and $^{2}J_{PP'}$ = 19.0 Hz (Figure 4). This $^{2}J_{PP'}$ coupling of 19.0 Hz was also used to successfully simulate the $^{13}C\{^{1}H\}$ NMR signals of **4** (see Supporting Information Figures S25 and S26), further supporting this value for $^{2}J_{PP'}$.

Also of note are the ^{29}Si satellites in the $^{31}P\{^{1}H\}$ NMR spectra of **2**–**4**. While **2** and **4** show apparent ^{29}Si satellites, the measured coupling from these satellite peaks does not match that found in the $^{29}Si\{^{1}H\}$ NMR spectra. This is likely due to the presence of one spin-active ^{29}Si nucleus causing the two ^{31}P nuclei to become magnetically inequivalent such that the satellite signal is not a simple doublet. For **3**, the measured $^{2}J_{SiP}$ from the satellites does match the $^{29}Si\{^{1}H\}$ NMR spectrum, suggesting that the two P atoms are (closer to) magnetically equivalent in **3**. The $^{31}P\{^{1}H\}$ NMR signal for **4** (δ_P = −209 ppm) occurs significantly downfield of the signals for **2** or **3** (δ_P = −288 and −284 ppm, respectively), which is consistent with previously published group 12 bis(silylphosphanide) complexes.[54] The ^{113}Cd and ^{199}Hg NMR spectra of **3** and **4** both appear as triplets, with large couplings to phosphorus ($^{1}J_{CdP}$ = 350 Hz, $^{1}J_{HgP}$ = 408 Hz).

CONCLUSIONS

We present the first one-step synthesis of a source of the phosphanide anion $[P(Si^{i}Pr_3)_2]^-$, in the form of $NaP(Si^{i}Pr_3)_2$ (**1**). Complex **1** was obtained in a 42% isolated yield, far higher than that of the previously reported Li phosphanide $[(THF)LiP(Si^{i}Pr_3)_2]_2$, thereby offering a significantly improved route to this ligand for synthetic investigations. $[(THF)NaP(Si^{i}Pr_3)_2]$ (**1a**), obtained from the solvation of **1** in THF, was characterized by single-crystal X-ray diffraction. With this synthetically useful methodology for **1**, we were able to complex this sterically demanding phosphanide ligand to Zn, Cd, and Hg, affording the novel two-coordinate complexes **2**–**4**. Single-crystal X-ray diffraction revealed that complexes **2**–**4** all show significant deviations from linearity in the solid state, with DFT calculations suggesting that this is due to the steric demands of the ligand. $^{13}C\{^{1}H\}$ and $^{29}Si\{^{1}H\}$ NMR spectroscopy of these ligands revealed strong second-order effects, suggesting the presence of virtual coupling between the two ^{31}P nuclei in these complexes. These studies show that $[P(Si^{i}Pr_3)_2]^-$ is now an accessible bulky, monodentate, monoanionic ligand.

EXPERIMENTAL SECTION

General Materials and Methods. All products described were synthesized with the rigorous exclusion of air and water using standard air-sensitive-handling techniques, which included benchtop operations (Schlenk line) and glovebox techniques, under argon and nitrogen, respectively. Solvents (*iso*-hexane, diethyl ether, THF, toluene) were collected from the in-house dry-solvent towers, degassed, and stored over 3 Å molecular sieves. *n*-Hexane was purchased extra-dry over molecular sieves from Thermo Scientific Chemicals, degassed, and stored over a second batch of 3 Å molecular sieves. DME was dried over CaH_2, distilled, degassed, and stored over 3 Å molecular sieves. C_6D_6 was dried over potassium, deuterated pyridine-d_5 was dried over CaH_2, and THF-d_8 was dried over sodium; all of these were distilled, degassed, and stored over 3 Å molecular sieves in the glovebox prior to use.

Anaerobic samples for NMR spectroscopy were prepared using glovebox techniques and sealed in J. Young's tap-modified borosilicate glass NMR tubes. NMR data were collected on either a Bruker AV400, AV(III)400, or AV(III) 500 spectrometer. Chemical shifts are quoted in ppm relative to TMS (^{1}H, $^{13}C\{^{1}H\}$, $^{29}Si\{^{1}H\}$) or H_3PO_4 (85% in D_2O, ^{31}P, and $^{31}P\{^{1}H\}$). ^{113}Cd and ^{199}Hg NMR chemical shifts are quoted in ppm relative to $CdMe_2$ and $HgMe_2$,

https://doi.org/10.1021/acs.inorgchem.4c03134
Inorg. Chem. 2024, 63, 20286−20294

Table 1. Selected Bond Lengths (Å) and Angles (deg) for $M[P(Si^iPr_3)_2]_2$ (M = Zn (2), Cd (3), Hg (4))[a]

	2	2a	3	4
M1−P1	2.2291(3)	2.2309(4)	2.4213(7)	2.3946(5)
M1−P2	2.2234(4)	2.2562(4)	2.4216(7)	2.3930(5)
P1−Si1	2.2532(4)	2.2629(4)	2.2571(7)	2.2614(7)
P1−Si2	2.2537(4)	2.2550(5)	2.2487(7)	2.2657(8)
P2−Si3	2.2456(4)	2.2598(5)	2.2557(8)	2.2644(7)
P2−Si4	2.2479(4)	2.2527(4)	2.2570(6)	2.2541(8)
P1−M1−P2	168.747(12)	163.593(18)	169.215(19)	170.086(16)
Si1−P1−Si2	125.9(1)	120.9(1)	120.5(1)	119.5(2)*
				123.9(2)*
Si3−P2−Si4	123.0(1)	120.9(1)	121.6(1)	117.1(2)*
				124.1(2)*
∑° around P1	334.14(2)	337.05(13)	330.52(3)	325.73(3)
∑° around P2	339.76(2)	322.26(13)	324.87(3)	331.16(3)

[a]Complexes **2**, **3**, and **4** were crystallized from *n*-hexane. **2a** is a polymorph of **2** crystallized from diethyl ether. Values marked with an asterisk correspond to disorder-modeled components.

respectively, using 0.1 M $Cd(ClO_4)_2/D_2O$ and 1.0 M $Hg(ClO_4)_2/D_2O$ solutions as external calibrants.

Anaerobic mass spectrometry samples for **2** were prepared under an argon atmosphere by flame-sealing the sample inside glass capillaries. Each sample was then opened and introduced immediately to a Bruker Impact II spectrometer with an APCI II source and a Direct Insertion Probe.

ATR-IR of solid samples were collected using a Bruker *α* FTIR spectrometer, using a resolution of 2 cm^{-1}, a frequency range of 500−4000 cm^{-1}, and a spectral average of 32 scans. These spectra were collected inside a nitrogen-filled glovebox. A background of the atmosphere was obtained prior to each data collection.

Elemental microanalyses were performed on an Exeter Analytical CE-440 Elemental Analyzer with samples combusted at 975 °C prior to measurement.

Caution: cadmium and mercury compounds are highly toxic, and great care must be taken in their manipulation.

*Synthesis of NaP(Si^{i}Pr$_3$)$_2$ (**1**).* Na (1.50 g, 65.3 mmol) and red phosphorus (0.63 g, 20.3 mmol) were suspended in DME (150 mL), and naphthalene (100 mg, 0.8 mmol) was added. The solution was refluxed for 24 h. A solution of ^{i}Pr$_3$SiCl (12.2 g, 65.3 mmol) in DME (50 mL) was added dropwise to the Na_3P solution at room temperature. The resulting suspension was refluxed for a further 24 h before allowing to cool to room temperature. The suspension was filtered to remove insoluble impurities, and the solvent was removed *in vacuo*. The resulting residue was extracted with toluene (200 mL), causing the precipitation of **1** as a pyrophoric white solid, which was isolated by filtration (3.12 g, 8.5 mmol, 42%). It should be noted that samples of **1** contained trace impurities of secondary phosphine (^{i}Pr$_3$Si)$_2$PH. ^{1}H NMR (pyridine-d$_5$, 400 MHz): δ 1.49−1.44 (m, 42H, ^{i}Pr (C*H*$_3$)$_2$ and ^{i}Pr (C*H*)). ^{13}C{^{1}H} NMR (pyridine-d$_5$, 101 MHz): δ 22.5 (d, $^3J_{CP}$ = 3.7 Hz, *C*H$_3$), 18.4 (d, $^2J_{CP}$ = 9.9 Hz, *C*H). ^{31}P NMR (pyridine-d$_5$, 162 MHz): δ − 378.3 (s). ^{31}P{^{1}H} NMR (pyridine-d$_5$, 162 MHz): δ − 378.3 (s). ATR-FTIR ν_{max} (cm^{-1}) 2936 (br, CH), 2857 (br, CH), 1460 (s, CH), 1358 (w), 1070 (m), 1012 (s), 1008 (w), 990 (w), 876 (s), 650 (s), 621 (s), 556 (s), 513 (s).

*Synthesis of (THF)NaP(Si^{i}Pr$_3$)$_2$ (**1a**).* Single crystals of the THF adduct, $[(THF)NaP(Si^iPr_3)_2]_2$ (**1a**), were obtained by crystallization of **1** from benzene and THF at room temperature for 4 weeks (see Figure S2). ^{1}H NMR (THF-*d*$_8$, 400 MHz, 25 °C): δ 3.63−3.60 (m, 6H, THF C*H*$_2$ (2,5)), 1.79−1.77 (m, 6H, THF C*H*$_2$ (3,4)), 1.12−1.10 (m, 84H, ^{i}Pr (C*H*$_3$)$_2$ and ^{i}Pr (C*H*)). N.B. The integrals corresponding to bound THF in 1a are smaller than expected due to displacement by THF-*d*$_8$. ^{13}C{^{1}H} NMR (THF-*d*$_8$, 101 MHz, 25 °C): δ 20.0 (d, $^3J_{C-P}$ = 3.4 Hz, ^{i}Pr (CH$_3$)$_2$), 16.3 (d, $^2J_{C-P}$ = 9.9 Hz, ^{i}Pr (*C*H)). ^{31}P NMR (THF-*d*$_8$, 162 MHz, 25 °C): δ − 384.2 (s). ^{31}P{^{1}H} NMR (THF-*d*$_8$, 162 MHz, 25 °C): δ − 384.2 (s). Elemental analysis: calculated for $C_{44}H_{100}Na_2O_2P_2Si_4$ (880.61 g mol^{-1}): C 59.95; H 11.43; N 0.00%. Found: C 59.93; H 11.48; N 0.26%.

General Procedures for the Synthesis of Complexes 2−4. Under an argon atmosphere, the corresponding group 12 halide, MX_2 (MX_2 = $ZnCl_2$, CdI_2, $HgBr_2$) (0.227 mmol), and the sodium salt **1** (200 mg, 0.542 mmol) were suspended in diethyl ether (10 mL) and stirred at room temperature for 16 h. Diethyl ether was removed under reduced pressure, producing a white solid. To this, *n*-hexane (10 mL) was added, and the white suspension was filtered. The solvent of the colorless filtrate was removed under reduced pressure yielding the crude products. Crystals suitable for single-crystal X-ray diffraction were grown by recrystallization from *n*-hexane at −30 °C.

*Data for Zn[P(Si^{i}Pr$_3$)$_2$]$_2$ (**2**).* Colorless crystals (69.7 mg, 0.092 mmol, 41%). ^{1}H NMR (C_6D_6, 400 MHz, 25 °C): δ 1.29 (m, 84H, ^{i}Pr (C*H*$_3$)$_2$ and ^{i}Pr (C*H*)). ^{13}C{^{1}H} NMR (C_6D_6, 101 MHz, 25 °C): δ 19.8 (m, $^3J_{CP}$ = 3.6 Hz, ^{i}Pr (CH$_3$)$_2$), 16.5 (m, $^2J_{CP}$ = 10.7 Hz, ^{i}Pr (*C*H)). ^{29}Si{^{1}H} NMR (C_6D_6 99 MHz, 25 °C): δ 24.7 (d, $^1J_{Si-P}$ = 37.5 Hz). ^{31}P{^{1}H} NMR (C_6D_6, 162 MHz, 25 °C): δ − 287.8 (s). ATR-FTIR ν_{max} (cm^{-1}) 2941 (br), 2860 (s), 2811 (w), 1460 (s), 1379 (m), 1363 (m), 1224 (w), 1068 (m), 1013 (s), 986 (s), 916 (w), 877 (s), 657 (s), 630 (s), 555 (s), 507 (s). HRMS (APCI), *m*/*z*: $[M + H]^+$ calculated for $C_{36}H_{85}ZnP_2Si_4$: 755.4490, found: 755.4523 (error = 4.5 ppm). Elemental analysis: calculated for $C_{36}H_{84}ZnP_2Si_4$ (754.44 g mol^{-1}): C 57.14; H 11.19; N 0.00%. Found: C 56.63; H 11.18; N 0.20%.

A second polymorph of **2**, referred to as **2a**, was crystallized by slow evaporation from diethyl ether and was also characterized by single-crystal X-ray diffraction.

*Cd[P(Si^{i}Pr$_3$)$_2$]$_2$ (**3**).* Colorless crystals (52.3 mg, 0.065 mmol, 57%). ^{1}H NMR (C_6D_6, 400 MHz, 25 °C): δ 1.29−1.28 (m, 84H, ^{i}Pr (C*H*$_3$)$_2$ and ^{i}Pr (C*H*)). ^{13}C{^{1}H} NMR (C_6D_6, 101 MHz, 25 °C): δ 19.8 (m, $^3J_{CP}$ = 3.7 Hz, ^{i}Pr (CH$_3$)$_2$), 16.7 (m, $^2J_{CP}$ = 10.3 Hz, ^{i}Pr (*C*H)). ^{29}Si{^{1}H} NMR (C_6D_6, 99 MHz, 25 °C): δ 24.4 (d, $^1J_{SiP}$ = 48.2 Hz). ^{31}P{^{1}H} NMR (C_6D_6, 162 MHz, 25 °C): δ − 284.0 (s). ^{113}Cd NMR (C_6D_6, 89 MHz, 25 °C): δ 137.68 (t, $^1J_{CdP}$ = 350 Hz). ATR-FTIR ν_{max} (cm^{-1}) 2942 (br), 2862 (s), 2819 (w), 1459 (s), 1379 (m), 1363 (m), 1226 (w), 1069 (m), 1013 (s), 992 (s), 917 (w), 878 (s), 658 (s), 630 (s), 568 (s), 505 (s), 481 (s).

*Hg[P(Si^{i}Pr$_3$)$_2$]$_2$ (**4**).* Colorless crystals (67.6 mg, 0.076 mmol, 55%). ^{1}H NMR (C_6D_6, 500 MHz, 25 °C): δ 1.30 (s, 84H, ^{i}Pr (C*H*$_3$)$_2$ and ^{i}Pr (C*H*)). ^{13}C{^{1}H} NMR (C_6D_6, 126 MHz, 25 °C): δ 19.7 (m, $^3J_{CP}$ = 3.5 Hz, ^{i}Pr (CH$_3$)$_2$), 16.7 (m, $^2J_{CP}$ = 10.2 Hz, ^{i}Pr (*C*H)). ^{29}Si{^{1}H} NMR (C_6D_6, 99 MHz, 25 °C): δ 25.3 (m). ^{31}P{^{1}H} NMR (C_6D_6, 99 MHz, 25 °C): δ − 209.2 (s). ^{199}Hg NMR (C_6D_6, 90 MHz, 25 °C): δ 13.2 (t, $^1J_{HgP}$ = 407.7 Hz). ATR-FTIR ν_{max} (cm^{-1}) 2941 (br), 2862 (s), 1457 (s), 1379 (m), 1363 (m), 1226 (w), 1069 (m), 1015 (s), 988 (s), 917 (w), 878 (s), 659 (s), 630 (s), 571 (s), 534 (s), 507 (s), 485 (s).

Computational Methodology. Geometry optimizations were performed for the models **2**−**4** using coordinates derived from their

https://doi.org/10.1021/acs.inorgchem.4c03134
Inorg. Chem. 2024, 63, 20286−20294

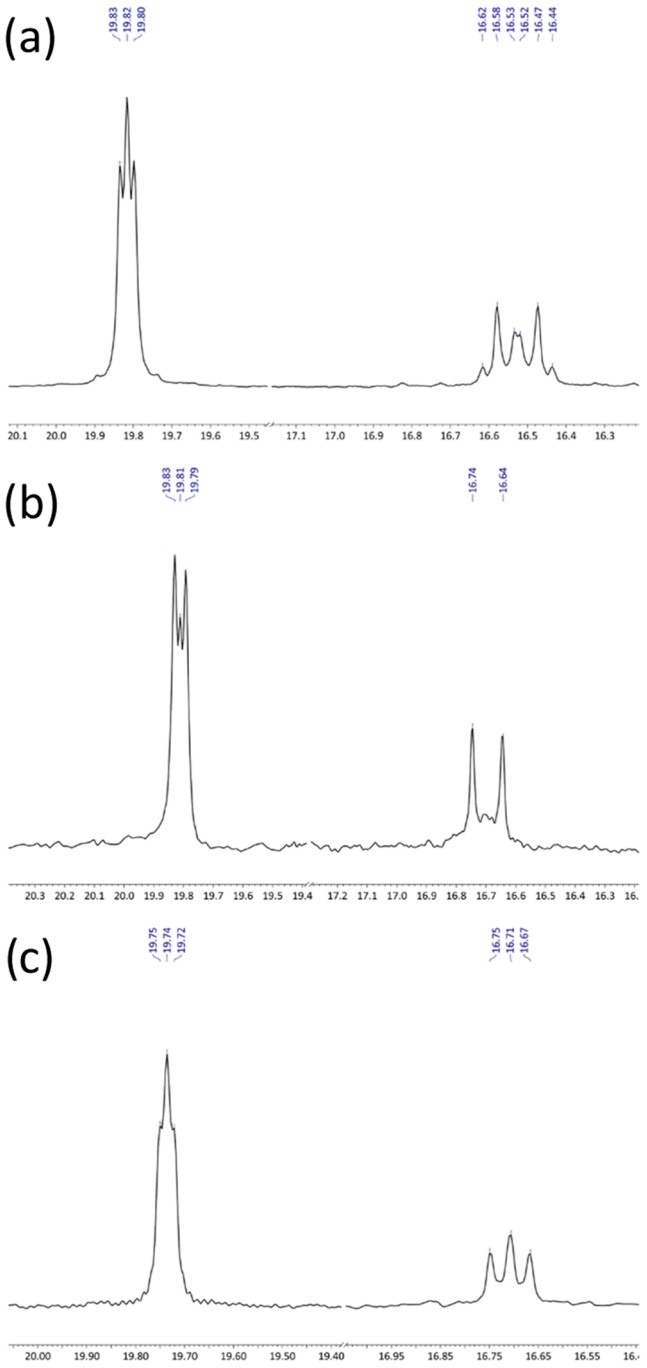

Figure 3. $^{13}C\{^{1}H\}$ NMR spectra of (a) **2**, (b) **3**, and (c) **4**, showing the extent of virtual coupling.

X-ray crystal structures. These models were geometry-optimized without restraints using the ORCA 5.0.4 software package[94] utilizing the PBE0 density functional[81,82] and all-electron ZORA-corrected[83] def2-TZVP basis sets[84−87] for all atoms (except Cd and Hg), SARC-ZORA-TZVP[88] basis sets for the Cd and Hg atoms, along with SARC/J auxiliary basis sets decontracted def2/J up to Kr[95] and SARC auxiliary basis sets beyond Kr.[88,96−98] Dispersion corrections were performed with Grimme's third-generation dispersion correction.[89,90] TightSCF and TightOpt convergence criteria were employed, and the location of true minima in these optimizations was confirmed by frequency analysis, which demonstrated that no imaginary vibrations were present.

Geometry optimizations for the linear analogues **2'**, **3'**, and **4'** were performed using coordinates derived from the X-ray crystal structure of $Cd[P(SiPh_3)_2]_2$.[54] These optimizations were carried out using the same methodology described above but with the P−M−P (M = Zn, Cd, Hg) angle constrained to 180°.

Two geometry optimizations were performed for $Cd[P(SiMe_3)_2]_2$, using coordinates derived from either the optimized structure of **2** (referred to as "bent" $Cd[P(SiMe_3)_2]_2$) or the optimized structure of **2'** (referred to as "linear" $Cd[P(SiMe_3)_2]_2$). The optimizations were conducted without restraints by using the same methodology described above. The "bent" and "linear" structures optimized to P−Cd−P bond angles of 177.5° and 179.9°, respectively, with the "bent" structure being $\Delta G = -0.1$ kcal mol^{-1} more stable.

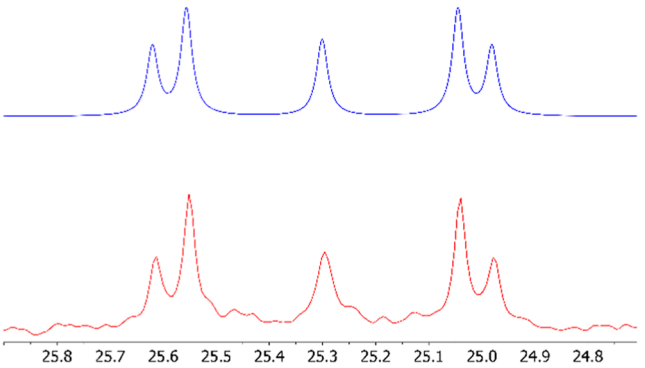

Figure 4. Experimental (red) and simulated (blue) $^{29}Si\{^{1}H\}$ NMR spectra of **4**, modeled using the parameters $^{1}J_{SiP} = 50.6$ Hz, $^{3}J_{SiP'} = 0.0$ Hz, and $^{2}J_{PP'} = 19.0$ Hz.

■ ASSOCIATED CONTENT

Supporting Information

The Supporting Information is available free of charge at https://pubs.acs.org/doi/10.1021/acs.inorgchem.4c03134.

Additional experimental details, materials and methods, HRMS spectra, IR spectra, NMR spectra, DFT calculations, and crystal data (PDF)
xyz files (ZIP)

Accession Codes

The CCDC (2372409−2372413) contains the supplementary crystallographic data for this paper. A data repository containing computational output files and spectroscopic data in their raw (NMR) and processed forms (IR, mass spectrometry, CHN) can be found via the following DOI: 10.17639/nott.7443. The initial draft of this manuscript has been deposited in ChemRxiv.[99]

■ AUTHOR INFORMATION

Corresponding Author

Deborah L. Kays − *School of Chemistry, University of Nottingham, Nottingham NG7 2RD, U.K.; School of Chemistry, Cardiff University, Cardiff CF10 3AT, U.K.;* orcid.org/0000-0002-4616-6001; Email: KaysD@cardiff.ac.uk

Authors

Olivia P. Churchill − *School of Chemistry, University of Nottingham, Nottingham NG7 2RD, U.K.*

Antonia Dase − *School of Chemistry, University of Nottingham, Nottingham NG7 2RD, U.K.*

Laurence J. Taylor − *School of Chemistry, University of Nottingham, Nottingham NG7 2RD, U.K.;* orcid.org/0000-0002-4948-4267

https://doi.org/10.1021/acs.inorgchem.4c03134
Inorg. Chem. 2024, 63, 20286−20294

Stephen P. Argent − *School of Chemistry, University of Nottingham, Nottingham NG7 2RD, U.K.;* orcid.org/0000-0002-3461-9675
Nathan T. Coles − *School of Chemistry, University of Nottingham, Nottingham NG7 2RD, U.K.*
Gavin S. Walker − *Advanced Materials Research Group, Faculty of Engineering, University of Nottingham, Nottingham NG7 2GA, U.K.;* orcid.org/0000-0001-5038-6923

Complete contact information is available at: https://pubs.acs.org/10.1021/acs.inorgchem.4c03134

Author Contributions

‖O.P.C. and A.D. contributed equally to this manuscript.

Notes

The authors declare no competing financial interest.

■ ACKNOWLEDGMENTS

The authors acknowledge the EPSRC [grant number EP/R004064/1; grant number EP/S023909/1], the Leverhulme Trust [grant number RPG-2021-183], and the University of Nottingham for financial support of this research. The authors thank Prof. David Mills and co-workers at the Department of Chemistry, University of Manchester, for invaluable chemical discussions regarding the synthesis of the $[P(Si^iPr_3)_2]^-$ complexes, the University of Nottingham Analytical Services Team for mass spectrometry, CHN microanalysis, and NMR spectroscopy measurements, and Dr Kevin Butler and Dr Huw Williams at the University of Nottingham for advice on simulating NMR spectra. The authors are also grateful for access to the University of Nottingham's Ada High Performance Computing Service.

■ REFERENCES

(1) Noor, A. Recent Developments in Two Coordinate Transition Metal Chemistry. *Coord. Chem. Rev.* **2023**, *476*, No. 214941.
(2) Kays, D. L. Extremely Bulky Amide Ligands in Main Group Chemistry. *Chem. Soc. Rev.* **2016**, *45* (4), 1004−1018.
(3) Taylor, L. J.; Kays, D. L. Low-Coordinate First-Row Transition Metal Complexes in Catalysis and Small Molecule Activation. *Dalton Trans.* **2019**, *48* (33), 12365−12381.
(4) Power, P. P. Some Highlights from the Development and Use of Bulky Monodentate Ligands. *J. Organomet. Chem.* **2004**, *689* (24), 3904−3919.
(5) Power, P. P. Stable Two-Coordinate, Open-Shell (d^1−d^9) Transition Metal Complexes. *Chem. Rev.* **2012**, *112* (6), 3482−3507.
(6) Goodwin, C. A. P.; Mills, D. P. Silylamides: Towards a Half-Century of Stabilising Remarkable f-Element Chemistry. In *Organometallic Chemistry*; Fairlamb, I.; Lynam, J. M.; Patmore, N. J.; Elliott, P., Eds.; The Royal Society of Chemistry, 2017; Vol. *41*, pp 123−156.
(7) Ortu, F.; Mills, D. P. Low-Coordinate Rare-Earth and Actinide Complexes. In *Handbook on the Physics and Chemistry of Rare Earths*; Bünzli, J.-C. G.; Pecharsky, V. K., Eds.; Elsevier, 2019; Vol. *55*, Chapter 306, pp 1−87.
(8) Shan, C.; Yao, S.; Driess, M. Where Silylene−Silicon Centres Matter in the Activation of Small Molecules. *Chem. Soc. Rev.* **2020**, *49* (18), 6733−6754.
(9) Webster, R. L. *β*-Diketiminate Complexes of the First Row Transition Metals: Applications in Catalysis. *Dalton Trans.* **2017**, *46* (14), 4483−4498.
(10) Lipschutz, M. I.; Chantarojsiri, T.; Dong, Y.; Tilley, T. D. Synthesis, Characterization, and Alkyne Trimerization Catalysis of a Heteroleptic Two-Coordinate FeI Complex. *J. Am. Chem. Soc.* **2015**, *137* (19), 6366−6372.
(11) Ung, G.; Rittle, J.; Soleilhavoup, M.; Bertrand, G.; Peters, J. C. Two-Coordinate Fe^0 and Co^0 Complexes Supported by Cyclic (Alkyl)(Amino)Carbenes. *Angew. Chem., Int. Ed.* **2014**, *53* (32), 8427−8431.
(12) Zimmermann, P.; Limberg, C. Activation of Small Molecules at Nickel(I) Moieties. *J. Am. Chem. Soc.* **2017**, *139* (12), 4233−4242.
(13) Roy, L.; Al-Afyouni, M. H.; DeRosha, D. E.; Mondal, B.; DiMucci, I. M.; Lancaster, K. M.; Shearer, J.; Bill, E.; Brennessel, W. W.; Neese, F.; Ye, S.; Holland, P. L. Reduction of CO_2 by a Masked Two-Coordinate Cobalt(I) Complex and Characterization of a Proposed Oxodicobalt(II) Intermediate. *Chem. Sci.* **2019**, *10* (3), 918−929.
(14) Lei, H.; Ellis, B. D.; Ni, C.; Grandjean, F.; Long, G. J.; Power, P. P. An Arene-Stabilized Cobalt(I) Aryl: Reactions with CO and NO. *Inorg. Chem.* **2008**, *47* (22), 10205−10207.
(15) Sharpe, H. R.; Geer, A. M.; Taylor, L. J.; Gridley, B. M.; Blundell, T. J.; Blake, A. J.; Davies, E. S.; Lewis, W.; McMaster, J.; Robinson, D.; Kays, D. L. Selective Reduction and Homologation of Carbon Monoxide by Organometallic Iron Complexes. *Nat. Commun.* **2018**, *9* (1), No. 3757.
(16) Lipschutz, M. I.; Tilley, T. D. Carbon−Carbon Cross-Coupling Reactions Catalyzed by a Two-Coordinate Nickel(II)−Bis(Amido) Complex via Observable Ni^I, Ni^{II}, and Ni^{III} Intermediates. *Angew. Chem., Int. Ed.* **2014**, *53* (28), 7290−7294.
(17) Sharpe, H. R.; Geer, A. M.; Lewis, W.; Blake, A. J.; Kays, D. L. Iron(II)-Catalyzed Hydrophosphination of Isocyanates. *Angew. Chem., Int. Ed.* **2017**, *56* (17), 4845−4848.
(18) Randall McClain, K.; Gould, C. A.; Chakarawet, K.; Teat, S. J.; Groshens, T. J.; Long, J. R.; Harvey, B. G. High-Temperature Magnetic Blocking and Magneto-Structural Correlations in a Series of Dysprosium(III) Metallocenium Single-Molecule Magnets. *Chem. Sci.* **2018**, *9* (45), 8492−8503.
(19) Guo, F.-S.; Day, B. M.; Chen, Y.-C.; Tong, M.-L.; Mansikkamäki, A.; Layfield, R. A. Magnetic Hysteresis up to 80 K in a Dysprosium Metallocene Single-Molecule Magnet. *Science* **2018**, *362* (6421), 1400−1403.
(20) Parmar, V. S.; Mills, D. P.; Winpenny, R. E. P. Mononuclear Dysprosium Alkoxide and Aryloxide Single-Molecule Magnets. *Chem. Eur. J.* **2021**, *27* (28), 7625−7645.
(21) Gould, C. A.; McClain, K. R.; Reta, D.; Kragskow, J. G. C.; Marchiori, D. A.; Lachman, E.; Choi, E.-S.; Analytis, J. G.; Britt, R. D.; Chilton, N. F.; Harvey, B. G.; Long, J. R. Ultrahard Magnetism from Mixed-Valence Dilanthanide Complexes with Metal-Metal Bonding. *Science* **2022**, *375* (6577), 198−202.
(22) Castellanos, E.; Benner, F.; Demir, S. Linear, Electron-Rich Erbium Single-Molecule Magnet with Dibenzocyclooctatetraene Ligands. *Inorg. Chem.* **2024**, *63* (21), 9888−9898.
(23) Bunting, P. C.; Atanasov, M.; Damgaard-Møller, E.; Perfetti, M.; Crassee, I.; Orlita, M.; Overgaard, J.; van Slageren, J.; Neese, F.; Long, J. R. A Linear Cobalt(II) Complex with Maximal Orbital Angular Momentum from a Non-Aufbau Ground State. *Science* **2018**, *362* (642), eaat7319.
(24) Zadrozny, J. M.; Xiao, D. J.; Atanasov, M.; Long, G. J.; Grandjean, F.; Neese, F.; Long, J. R. Magnetic Blocking in a Linear Iron(I) Complex. *Nat. Chem.* **2013**, *5* (7), 577−581.
(25) Zadrozny, J. M.; Atanasov, M.; Bryan, A. M.; Lin, C.-Y.; Rekken, B. D.; Power, P. P.; Neese, F.; Long, J. R. Slow Magnetization Dynamics in a Series of Two-Coordinate Iron(II) Complexes. *Chem. Sci.* **2013**, *4* (1), 125−138.
(26) Yao, X.-N.; Du, J.-Z.; Zhang, Y.-Q.; Leng, X.-B.; Yang, M.-W.; Jiang, S.-D.; Wang, Z.-X.; Ouyang, Z.-W.; Deng, L.; Wang, B.-W.; Gao, S. Two-Coordinate Co(II) Imido Complexes as Outstanding Single-Molecule Magnets. *J. Am. Chem. Soc.* **2017**, *139* (1), 373−380.
(27) Valentine, A. J.; Geer, A. M.; Blundell, T. J.; Tovey, W.; Cliffe, M. J.; Davies, E. S.; Argent, S. P.; Lewis, W.; McMaster, J.; Taylor, L. J.; Reta, D.; Kays, D. L. Slow Magnetic Relaxation in Fe(II) *m*-Terphenyl Complexes. *Dalton Trans.* **2022**, *51* (47), 18118−18126.
(28) Bürger, H.; Wannagat, U. Silylamido-Derivate von Eisen und Kobalt. *Monatsh. Chem.* **1963**, *94* (6), 1007−1012.

(29) Bürger, H.; Wannagat, U. Silylamido-Verbindungen von Chrom, Mangan, Nickel und Kupfer. *Monatsh. Chem.* **1964**, *95* (4), 1099−1102.
(30) Bürger, H.; Sawodny, W.; Wannagat, U. Darstellung Und Schwinkungsspektren von Silylamiden Der Elemente Zink, Cadmium Und Quecksilber. *J. Organomet. Chem.* **1965**, *3* (2), 113−120.
(31) Wannagat, U.; Niederprüm, H. Beiträge zur Chemie der Silicium-Stickstoff-Verbindungen, XIII. Silylsubstituierte Alkaliamide. *Chem. Ber.* **1961**, *94* (6), 1540−1547.
(32) Sheldrick, G. M.; Sheldrick, W. S. Crystal and Molecular Structure of Tris[Bis(Trimethylsilyl)Amino]Aluminium, Al[N-$(SiMe_3)_2]_3$. *J. Chem. Soc. A* **1969**, No. 0, 2279−2282.
(33) Harris, D. H.; Lappert, M. F. Monomeric, Volatile Bivalent Amides of Group IVB Elements, $M(NR^1{}_2)_2$ and $M(NR^1R_2)_2$ (M = Ge, Sn, or Pb; R^1 = Me_3Si, R2 = Me_3C). *J. Chem. Soc., Chem. Commun.* **1974**, No. 21, 895−896.
(34) Schaeffer, C. D., Jr.; Zuckerman, J. J. Tin(II) Organosilylamines. *J. Am. Chem. Soc.* **1974**, *96* (22), 7160−7162.
(35) Waezsada, S. D.; Belgardt, T.; Noltemeyer, M.; Roesky, H. W. $2,6\text{-}^iPr_2C_6H_3(Me_3Si)NTl]_4$—A Covalent Thallium(I)-Nitrogen Compound with Weak Arene−Thallium Interactions. *Angew. Chem., Int. Ed.* **1994**, *33* (13), 1351−1352.
(36) Petrie, M. A.; Ruhlandt-Senge, K.; Power, P. P. Synthesis and Characterization of the Monomeric Aluminum Monoamides (*tert*-$Bu)_2AlN(R)R'$ (R and R′ = Bulky Aryl, Alkyl, or Silyl Groups). *Inorg. Chem.* **1993**, *32* (7), 1135−1141.
(37) Wraage, K.; Lameyer, L.; Stalke, D.; Roesky, H. W. Reaction of $RGeBr_3$ (R = $^iPr_2C_6H_3NSiMe_3$) with Ammonia To Give $(RGe)_2(NH_2)_4(NH)$: A Compound Containing Terminal NH_2 Groups. *Angew. Chem., Int. Ed.* **1999**, *38* (4), 522−523.
(38) Babcock, J. R.; Liable-Sands, L.; Rheingold, A. L.; Sita, L. R. Syntheses, Structural Characterizations, and Heterocumulene Metathesis Studies of New Monomeric Bis(Triorganosilylamido)Tin(II) Derivatives. *Organometallics* **1999**, *18* (21), 4437−4441.
(39) Brynda, M.; Herber, R.; Hitchcock, P. B.; Lappert, M. F.; Nowik, I.; Power, P. P.; Protchenko, A. V.; Růžička, A.; Steiner, J. Higher-Nuclearity Group 14 Metalloid Clusters: $[Sn_9Sn(NRR')_6]$. *Angew. Chem.* **2006**, *118* (26), 4439−4443.
(40) Lipschutz, M. I.; Tilley, T. D. Synthesis and Reactivity of a Conveniently Prepared Two-Coordinate Bis(Amido) Nickel(II) Complex. *Chem. Commun.* **2012**, *48* (57), 7146−7148.
(41) Deschner, T.; Klimpel, M.; Tafipolski, M.; Scherer, W.; Törnroos, K.; Anwander, R. Postfunctionalization of Periodic Mesoporous Silica SBA-1 with Magnesium(II) and Iron(II) Silylamides. *Dalton Trans.* **2012**, *41*, 7319−7326.
(42) Lin, C.-Y.; Guo, J.-D.; Fettinger, J. C.; Nagase, S.; Grandjean, F.; Long, G. J.; Chilton, N. F.; Power, P. P. Dispersion Force Stabilized Two-Coordinate Transition Metal−Amido Complexes of the $-N(SiMe_3)$Dipp (Dipp = $C_6H_3\text{-}2,6\text{-}Pr^i{}_2$) Ligand: Structural, Spectroscopic, Magnetic, and Computational Studies. *Inorg. Chem.* **2013**, *52* (23), 13584−13593.
(43) Coles, M. P. The Role of the *Bis*-Trimethylsilylamido Ligand, $[N\{SiMe_3\}_2]^-$, in Main Group Chemistry. Part 1: Structural Chemistry of the *s*-Block Elements. *Coord. Chem. Rev.* **2015**, *297*−*298*, 2−23.
(44) Coles, M. P. The Role of the *Bis*-Trimethylsilylamido Ligand, $[N\{SiMe_3\}_2]^-$, in Main Group Chemistry. Part 2: Structural Chemistry of the Metallic *p*-Block Elements. *Coord. Chem. Rev.* **2015**, *297*−*298*, 24−39.
(45) Goodwin, C. A. P.; Chilton, N. F.; Vettese, G. F.; Moreno Pineda, E.; Crowe, I. F.; Ziller, J. W.; Winpenny, R. E. P.; Evans, W. J.; Mills, D. P. Physicochemical Properties of Near-Linear Lanthanide(II) Bis(Silylamide) Complexes (Ln = Sm, Eu, Tm, Yb). *Inorg. Chem.* **2016**, *55* (20), 10057−10067.
(46) Chilton, N. F.; Goodwin, C. A. P.; Mills, D. P.; Winpenny, R. E. P. The First Near-Linear Bis(Amide) f-Block Complex: A Blueprint for a High Temperature Single Molecule Magnet. *Chem. Commun.* **2015**, *51* (1), 101−103.
(47) Goodwin, C. A. P.; Chilton, N. F.; Natrajan, L. S.; Boulon, M.-E.; Ziller, J. W.; Evans, W. J.; Mills, D. P. Investigation into the Effects of a Trigonal-Planar Ligand Field on the Electronic Properties of Lanthanide(II) Tris(Silylamide) Complexes (Ln = Sm, Eu, Tm, Yb). *Inorg. Chem.* **2017**, *56* (10), 5959−5970.
(48) Thum, K.; Martin, J.; Elsen, H.; Eyselein, J.; Stiegler, L.; Langer, J.; Harder, S. Lewis Acidic Cationic Strontium and Barium Complexes. *Eur. J. Inorg. Chem.* **2021**, *2021* (26), 2643−2653.
(49) Knüpfer, C.; Klerner, L.; Mai, J.; Langer, J.; Harder, S. S-Block Metal Complexes of Superbulky $(^tBu_3Si)_2N^-$: A New Weakly Coordinating Anion? *Chem. Sci.* **2024**, *15* (12), 4386−4395.
(50) Goel, S. C.; Chiang, M. Y.; Buhro, W. E. Synthesis of Homoleptic Silylphosphido Complexes $(M[P(SiMe_3)_2][\mu\text{-}P(SiMe_3)_2])_2$, Where M = Zinc and Cadmium, and Their Use in Metalloorganic Routes to Cd_3P_2 and $MGeP_2$. *J. Am. Chem. Soc.* **1990**, *112* (14), 5636−5637.
(51) Hey, E.; Hitchcock, P. B.; Lappert, M. F.; Rai, A. K. Bis(Trimethylsilyl)Phosphidometal Complexes. I. Isolation and NMR Spectra of $Li_4(\mu_2\text{-}PR_2)_2(\mu_3\text{-}PR_2)_2(THF)_2$ (I), $Li(PR_2(PMDETA)$ (II), and X-Ray Structures of Compound I and $[Li(\mu\text{-}PR_2)(THF)_2]_2$ (III) (R = $SiMe_3$). *J. Organomet. Chem.* **1987**, *325* (1−2), 1−12.
(52) Hey-Hawkins, E.; Sattler, E. Crystal Structure of Solvent-Free Hexameric $LiP(SiMe_3)_2$: A Ladder with Six Li−P Steps. *J. Chem. Soc., Chem. Commun.* **1992**, No. 10, 775−776.
(53) Englich, U.; Hassler, K.; Ruhlandt-Senge, K.; Uhlig, F. A Convenient Synthetic Strategy toward Heavy Alkali Metal Bis(Trimethylsilyl)Phosphides: Crystal Structures of the Ladder-Type Polymers $[A(thf)P(SiMe_3)_2]_\infty$ (A = K, Rb, Cs). *Inorg. Chem.* **1998**, *37* (14), 3532−3537.
(54) Matchett, M. A.; Chiang, M. Y.; Buhro, W. E. Disilylphosphido Complexes $M[P(SiPh_3)_2]_2$, Where M = Zn, Cd, Hg, and Sn: Effective Steric Equivalency of $P(SiPh_3)_2$ and $N(SiMe_3)_2$ Ligands. *Inorg. Chem.* **1994**, *33* (6), 1109−1114.
(55) Schäfer, H.; Fritz, G.; Hölderich, W. Das $LiPH_2$ ·1 Monoglym. *Z. Anorg. Allg. Chem.* **1977**, *428* (1), 222−224.
(56) Baudler, M.; Glinka, K.; Jones, R. A. Trilithium Heptaphosphide, Dilithium Hexadecaphosphide, and Trisodium Henicosaphosphide. In *Inorganic Syntheses*; John Wiley & Sons, Ltd, 1990; pp 227−235.
(57) Westerhausen, M.; Löw, R.; Schwarz, W. NMR-Spektroskopische Und Strukturelle Charakterisierung Der Tri-*Iso*-Propylsilylphosphanide Des Calciums. *J. Organomet. Chem.* **1996**, *513* (1), 213−229.
(58) Westerhausen, M.; Rotter, T.; Görls, H.; Birg, C.; Warchhold, M.; Nöth, H. Lithium Bis(Triisopropylsilyl)Phosphanide and Its Pentacarbonyltungsten Adduct: Synthesis and Crystal Structures of the Dimer $[(Thf)Li\text{-}P(Si^iPr_3)_2]_2$ and the Solvent-Separated Ion Pair $[(Thf)_4Li]^+[(OC)_5W\text{-}P(Si^iPr_3)_2]^-$. *Z. Naturforsch. B* **2005**, *60* (7), 766−770.
(59) von Hänisch, C. Die Tris(Triisopropylsilyl)Pnikogene: Synthese Und Charakterisierung von $[E(SiPr_3)_3]$ (E = P, As, Sb). *Z. Anorg. Allg. Chem.* **2001**, *627* (7), 1414−1416.
(60) Gary, D. C.; Cossairt, B. M. Role of Acid in Precursor Conversion During InP Quantum Dot Synthesis. *Chem. Mater.* **2013**, *25* (12), 2463−2469.
(61) Bürger, H.; Goetze, U. Die Hydrolytische Spaltung von Tris(Trimethylsilyl)Derivaten Der Elemente Phosphor, Arsen Und Antimon. *J. Organomet. Chem.* **1968**, *12* (3), 451−457.
(62) Connelly, N. G.; Geiger, W. E. Chemical Redox Agents for Organometallic Chemistry. *Chem. Rev.* **1996**, *96* (2), 877−910.
(63) Le Corre, G.; Grützmacher, H. Simple Conversion of Trisodium Phosphide, Na_3P, into Silyl- and Cyanophosphides and the Structure of a Terminal Silver Phosphide. *Dalton Trans.* **2022**, *51* (9), 3497−3501.
(64) Jupp, A. R.; Goicoechea, J. M. The 2-Phosphaethynolate Anion: A Convenient Synthesis and [2 + 2] Cycloaddition Chemistry. *Angew. Chem., Int. Ed.* **2013**, *52* (38), 10064−10067.
(65) Kamer, P. C. J.; van Leeuwen, P. W. N. M. *Phosphorus(III) Ligands in Homogeneous Catalysis: Design and Synthesis*, John Wiley & Sons, Incorporated: Newark, UNITED KINGDOM, 2012.

https://doi.org/10.1021/acs.inorgchem.4c03134
Inorg. Chem. 2024, 63, 20286−20294

(66) Baldwin, J.; Brookfield, A.; Whitehead, G. F. S.; Natrajan, L. S.; McInnes, E. J. L.; Oakley, M. S.; Mills, D. P. Synthesis and Characterization of Solvated Lanthanide (II) Bis(Triisopropylsilyl)-Phosphide Complexes. *ChemRxiv*, 2024 DOI: 10.26434/chemrxiv-2024-3m17t.
(67) Nesterov, V.; Breit, N. C.; Inoue, S. Advances in Phosphasilene Chemistry. *Chem. Eur. J.* **2017**, *23* (50), 12014−12039.
(68) King, R. B. Atomic Orbitals, Symmetry, and Coordination Polyhedra. *Coord. Chem. Rev.* **2000**, *197* (1), 141−168.
(69) Cole, S. C.; Coles, M. P.; B Hitchcock, P. Dimesitylzinc : A Strictly 2-Coordinate, Homoleptic Diarylzinc Compound. *Dalton Trans.* **2003**, *0* (19), 3663−3664.
(70) Fox, B. S.; Beyer, M. K.; Bondybey, V. E. Coordination Chemistry of Silver Cations. *J. Am. Chem. Soc.* **2002**, *124* (45), 13613−13623.
(71) Margraf, G.; Lerner, H.-W.; Bolte, M.; Wagner, M. Kristallstruktur Des Zinkamids Zn[N(SiMe3)2]2. *Z. Anorg. Allg. Chem.* **2004**, *630* (2), 217−218.
(72) Chisholm, M. H.; Gallucci, J. C.; Yin, H.; Zhen, H. Arylzinc Alkoxides: [ArZnOCHP]2 and Ar2Zn3(OCHP)4 When Ar = C6H5, p-CF3C6H4, 2,4,6-Me3C6H2, and C6F5. *Inorg. Chem.* **2005**, *44* (13), 4777−4785.
(73) Schröder, A.; Lork, E.; Beckmann, J. Synthesis and Structure of Bis(m-Terphenyl)Zinc (2,6-Mes2 C6 H3)2 Zn. *Main Group Met. Chem.* **2014**, *37* (5−6), 155−157.
(74) Blundell, T. J.; Hastings, F. R.; Gridley, B. M.; Moxey, G. J.; Lewis, W.; Blake, A. J.; Kays, D. L. Ligand Influences on Homoleptic Group 12 *m*-Terphenyl Complexes. *Dalton Trans.* **2014**, *43* (38), 14257−14264.
(75) Krieck, S.; Görls, H.; Westerhausen, M. Bis(2,4,6-Trimethylphenyl)Zinc(II). *Acta Crystallogr. E: Structure Rep. Online* **2009**, *65* (7), m809.
(76) Valentine, A. J.; Taylor, L. J.; Geer, A. M.; Huke, C. D.; Wood, K. E.; Tovey, W.; Lewis, W.; Argent, S. P.; Teale, A. M.; McMaster, J.; Kays, D. L. Structural and Electronic Studies of Substituted *m*-Terphenyl Group 12 Complexes. *Organometallics* **2022**, *41* (11), 1426−1433.
(77) Linearization energy is the computed Gibbs free energy of the linear complex relative to the (bent) equilibrium geometry, see Wolters, L. P.; Bickelhaupt, F. M. Nonlinear d^{10}-ML_2 Transition-Metal Complexes. *ChemistryOpen* **2013**, *2* (3), 106−114.
(78) Brooker, S.; Bertel, N.; Stalke, D.; Noltemeyer, M.; Roesky, H. W.; Sheldrick, G. M.; Edelmann, F. T. Main-Group Chemistry of the 2,4,6-Tris(Trifluoromethyl)Phenyl Substituent: X-Ray Crystal Structures of $[2,4,6\text{-}(CF_3)_3C_6H_2]_2Zn$, $[2,4,6\text{-}(CF_3)_3C_6H_2]_2Cd(MeCN)$ and $[2,4,6\text{-}(CF_3)_3C_6H_3]_2Hg$. *Organometallics* **1992**, *11* (1), 192−195.
(79) Gridley, B. M.; Moxey, G. J.; Lewis, W.; Blake, A. J.; Kays, D. L. Conformational Isomerism in Monomeric, Low-Coordinate Group 12 Complexes Stabilized by a Naphthyl-Substituted m-Terphenyl Ligand. *Chem. Eur. J.* **2013**, *19* (34), 11446−11453.
(80) Westerhausen, M.; Oßberger, M. W.; Alexander, J. S.; Ruhlandt-Senge, K. Influence of the Steric Demand of the 2,4,6-Trialkylphenyl Substituents on the Structures and Reactivity of Diarylzinc. *Z. Anorg. Allg. Chem.* **2005**, *631* (13−14), 2836−2841.
(81) Perdew, J. P.; Burke, K.; Ernzerhof, M. Generalized Gradient Approximation Made Simple. *Phys. Rev. Lett.* **1996**, *77* (18), 3865−3868.
(82) Adamo, C.; Barone, V. Toward Reliable Density Functional Methods without Adjustable Parameters: The PBE0Model. *J. Chem. Phys.* **1999**, *110* (13), 6158−6170.
(83) van Lenthe, E.; Snijders, J. G.; Baerends, E. J. The Zero-order Regular Approximation for Relativistic Effects: The Effect of Spin−Orbit Coupling in Closed Shell Molecules. *J. Chem. Phys.* **1996**, *105* (15), 6505−6516.
(84) Weigend, F.; Furche, F.; Ahlrichs, R. Gaussian Basis Sets of Quadruple Zeta Valence Quality for Atoms H−Kr. *J. Chem. Phys.* **2003**, *119* (24), 12753−12762.
(85) Schäfer, A.; Horn, H.; Ahlrichs, R. Fully Optimized Contracted Gaussian Basis Sets for Atoms Li to Kr. *J. Chem. Phys.* **1992**, *97* (4), 2571−2577.
(86) Schäfer, A.; Huber, C.; Ahlrichs, R. Fully Optimized Contracted Gaussian Basis Sets of Triple Zeta Valence Quality for Atoms Li to Kr. *J. Chem. Phys.* **1994**, *100* (8), 5829−5835.
(87) Weigend, F.; Ahlrichs, R. Balanced Basis Sets of Split Valence, Triple Zeta Valence and Quadruple Zeta Valence Quality for H to Rn: Design and Assessment of Accuracy. *Phys. Chem. Chem. Phys.* **2005**, *7* (18), 3297−3305.
(88) Pantazis, D. A.; Chen, X.-Y.; Landis, C. R.; Neese, F. All-Electron Scalar Relativistic Basis Sets for Third-Row Transition Metal Atoms. *J. Chem. Theory Comput.* **2008**, *4* (6), 908−919.
(89) Grimme, S.; Antony, J.; Ehrlich, S.; Krieg, H. A Consistent and Accurate Ab Initio Parametrization of Density Functional Dispersion Correction (DFT-D) for the 94 Elements H-Pu. *J. Chem. Phys.* **2010**, *132* (15), No. 154104.
(90) Goerigk, L.; Grimme, S. A Thorough Benchmark of Density Functional Methods for General Main Group Thermochemistry, Kinetics, and Noncovalent Interactions. *Phys. Chem. Chem. Phys.* **2011**, *13* (14), 6670−6688.
(91) Pidcock, A. Coupling and "Virtual" Coupling in the Nuclear Magnetic Resonance Spectra of Phosphine Complexes. *Chem. Commun.* **1968**, *0* (2), 92.
(92) Hersh, W. H. False AA'X Spin-Spin Coupling Systems in ^{13}C NMR: Examples Involving Phosphorus and a 20-Year-Old Mystery in Off-Resonance Decoupling. *J. Chem. Educ.* **1997**, *74* (12), 1485.
(93) Verstuyft, A. W.; Nelson, J. H.; Cary, L. W. Investigation of the Utility of "Virtual Coupling" in the $^{13}C\{^1H\}$ Nuclear Magnetic Resonance Spectra of Bis-Phosphite Complexes of Palladium and Platinum. Algebraic Cancelation of Spin-Spin Coupling. *Inorg. Chem.* **1976**, *15* (3), 732−734.
(94) Neese, F. Software Update: The ORCA Program System—Version 5.0. *WIREs Comput. Mol. Sci.* **2022**, *12* (5), e1606 DOI: 10.1002/wcms.1606.
(95) Weigend, F. Accurate Coulomb-Fitting Basis Sets for H to Rn. *Phys. Chem. Chem. Phys.* **2006**, *8* (9), 1057−1065.
(96) Pantazis, D. A.; Neese, F. All-Electron Scalar Relativistic Basis Sets for the Lanthanides. *J. Chem. Theory Comput.* **2009**, *5* (9), 2229−2238.
(97) Pantazis, D. A.; Neese, F. All-Electron Scalar Relativistic Basis Sets for the Actinides. *J. Chem. Theory Comput.* **2011**, *7* (3), 677−684.
(98) Pantazis, D. A.; Neese, F. All-Electron Scalar Relativistic Basis Sets for the 6p Elements. *Theor. Chem. Acc.* **2012**, *131* (11), 1292.
(99) Churchill, O. P.; Dase, A.; Taylor, L. J.; Argent, S. P.; Coles, N. T.; Walker, G. S.; Kays, D. L. Synthesis of the bulky phosphanide $(^iPr_3Si)_2P^-$ and its stabilisation of low-coordinate group 12 complexes *ChemRxiv* 2024, DOI: 10.26434/chemrxiv-2024-f4lkp.

https://doi.org/10.1021/acs.inorgchem.4c03134
Inorg. Chem. 2024, 63, 20286−20294